UV studies of electron impact excitation of CS2

J. M. Ajello and S. K. Srivastava

Citation: The Journal of Chemical Physics **75**, 4454 (1981); doi: 10.1063/1.442612
View online: http://dx.doi.org/10.1063/1.442612
View Table of Contents: http://scitation.aip.org/content/aip/journal/jcp/75/9?ver=pdfcov
Published by the AIP Publishing

UV studies of electron impact excitation of CS_2 [a)]

J. M. Ajello and S. K. Srivastava

Jet Propulsion Laboratory, California Institute of Technology, Pasadena, California 91109
(Received 28 April 1981; accepted 30 June 1981)

We report the first measurements of emission cross sections of CS_2 by electron impact over the wavelength interval 110 to 510 nm. Absolute emission cross sections are obtained at 100 eV for all spectral features observed in the interval. The important electronic transitions listed in decreasing order of their emission cross sections at 100 eV are the ionization transitions $CS_2^+(\tilde{B}\,^2\Sigma_u^+ \rightarrow \tilde{X}\,^2\Pi_g)$ in the middle UV, $CS_2^+(\tilde{A}\,^2\Pi_u \rightarrow \tilde{X}\,^2\Pi_g)$ in the visible, the dissociative excitation transition $CS(A\,^1\Pi \rightarrow X\,^1\Sigma^+)$ in the middle UV, and individual carbon and sulfur multiplets in the VUV. Emission cross sections as a function of electron energy (0–125 eV) are reported for several of the important electronic transitions.

I. INTRODUCTION

The recent identification of CS, C, and S emissions in the UV spectra of comets[1–3] has necessitated the investigation of the stable parent molecule(s) of these atomic and radical species, e. g., CS_2 and/or COS. This prompted us to study the fluorescence spectra of CS_2 by electron impact. The goals of the study are threefold: (1) demonstrate the capability of a new experimental apparatus for recording electron impact induced fluorescence spectra and for measuring emission cross sections; (2) identify important emission spectral features resulting from the inelastic collisional process $CS_2 + e$, and for these features measure the relevant emission cross sections; and (3) compare the resulting emission spectra with cometary spectra and previous laboratory data.

At the present time, for CS_2, there has not been any electron impact study for the observed spectral features.[4,5] Our measurements show that the spectral features produced are predominantly of two types: (1) atomic lines of C and S in the VUV, and (2) ionic bands of CS_2 in the middle UV and visible with, additionally, a small amount of CS emission in the middle UV.

The last few years have been extremely productive for the understanding of the spectroscopy of CS_2. The most important recent works were the high resolution studies which identified the vibrational structure of the strong and dominant $CS_2^+(\tilde{A}\,^2\Pi_u, \tilde{B}\,^2\Sigma_u^+ \rightarrow \tilde{X}\,^2\Pi_g)$ ionic transitions.[4,6] Of equal importance in understanding the spectroscopy of CS_2 and in particular for locating excited states on an energy level diagram are the precise photoionization measurements of the first ionization potential of CS_2 by Ono *et al.*[7] Previous photoionization measurements by Dibeler and Walker[8] give an idea as to the ionization fragmentation processes expected from electron impact.

Additionally, recent experimental data from laser induced fluorescence spectra have been important in determining vibrational frequencies[9] and the internal energy distribution of photodissociative products.[10,11] From earlier works, fluorescence induced spectra obtained by Lee and Judge[12] and Lee *et al.*[13] by photon impact were extremely helpful in the interpretation of the detailed results of the electron impact experiment presented here.

In Sec. II the experimental apparatus and method are presented, in Sec. III the results are given, and in Sec. IV these results are discussed.

II. APPARATUS AND METHOD

A. Apparatus

The apparatus used for the present measurements is shown in Fig. 1. It consists of an electron collision chamber in tandem with a UV/visible spectrometer. A collimated beam of electrons, whose energy can be varied from 1 eV to 1 keV is generated by a magnetically collimated electron gun.[14] The energy spread of the electron beam is estimated to be about 0. 5 eV full width at half-maximum (FWHM) and the absolute accuracy of the energy scale to be within 1 eV. This beam of electrons is made to collide with a target beam of atoms or molecules. The two beams intersect at 90°. Alternatively, the vacuum chamber of the scattering spectrometer can be filled up by the desired gas to the required pressure and the beam of electrons is made to pass through it. For the purpose of discussion here, the former collision geometry will be referred to as "crossed beam" and the latter as the "static gas" geometry.

As a result of collisions, photons are generated. At an angle θ with respect to the electron beam, the photons enter into the UV/visible spectrometer. Normally, the angle θ is fixed either at 90° or 54. 4° (the magic angle). However, any other direction of observation can be chosen. The spectrometer is fitted with a 20 cm focal length concave holographic grating. At the exit slit of the spectrometer various photon detectors with different spectral sensitivity regions are placed. Since the emitted photon intensity is generally low, photon counting methods are employed. The output signals from the photon detectors are amplified and are stored as a function of wavelength or electron impact energy in a multichannel analyzer.

In the following, the various components of the experimental arrangement are described in detail.

[a] This work was supported by the Planetary Atmospheres, Astronomy/Relativity and Laser Kinetics Programs of NASA. It represents one phase of work sponsored by NASA under Contract NAS7-100 to the Jet Propulsion Laboratory, California Institute of Technology, Pasadena, Cal. 91109.

 0021-9606/81/214454-10$01.00

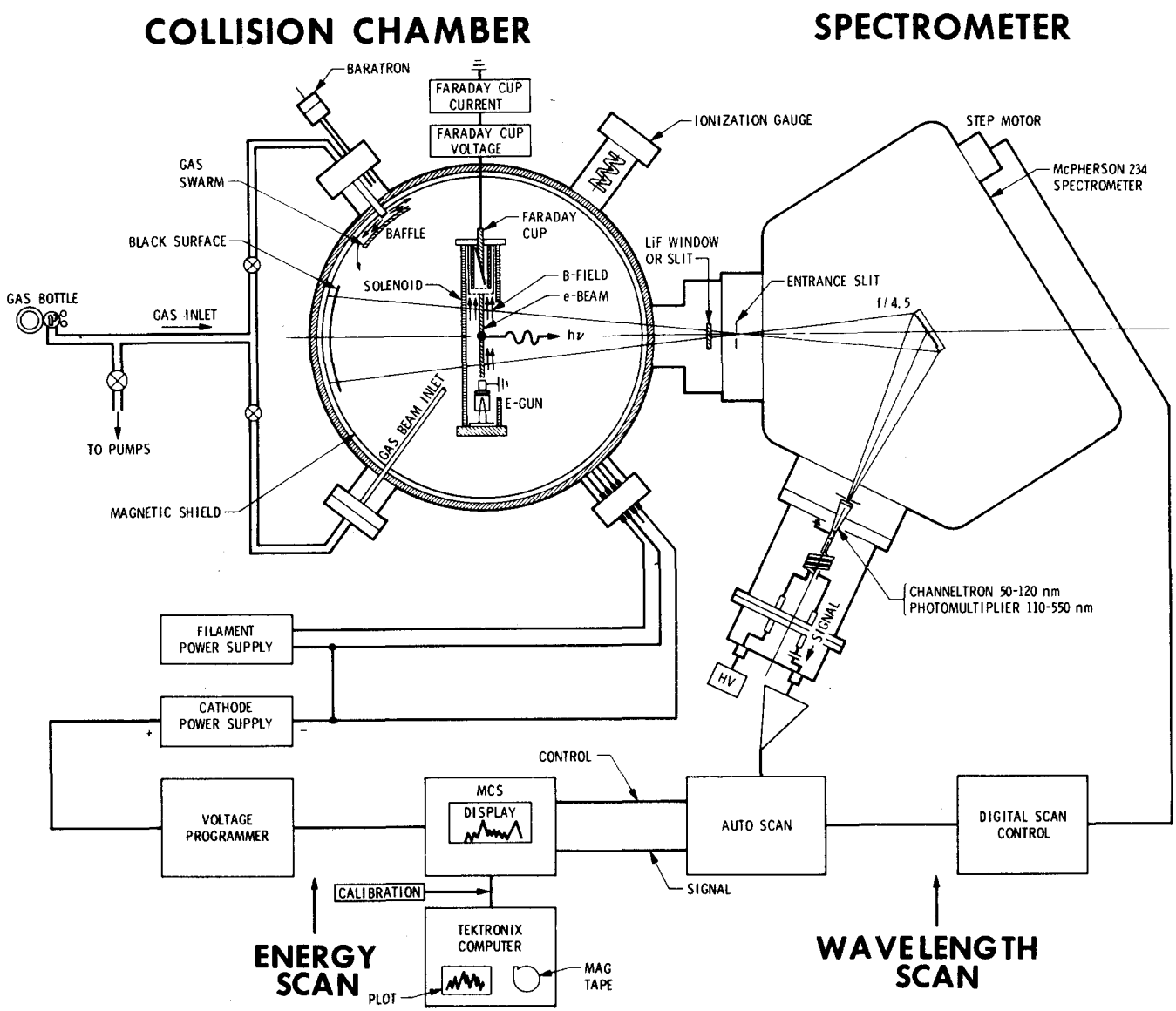

FIG. 1. Schematic diagram of the "electron impact emission spectrometer."

1. *Electron collision chamber*

This chamber is a stainless steel vacuum chamber which is 2 ft high and 14 in. in diameter. The vacuum chamber is lined with a μ-metal shield which reduces the external magnetic field to less than 20 mG. It has 16 vacuum ports through which the various electrical feedthroughs, pressure sensors, and other peripherals can be connected to the spectrometer. The chamber is pumped by a 1500 liter/sec high speed oil diffusion and mechanical pump system. The vacuum port through which the diffusion pump is connected to the vacuum chamber is fitted with a micrometer adjustable variable orifice to control the pumping speed at the collision chamber. The pressure in the chamber is measured by a thermocouple gauge, an ionization gauge, and a MKS baratron. The thermocouple gauge provides the pressure readings during the roughing stage. The ionization gauge is used as a general pressure monitor during the normal operation. The MKS baratron is used for accurate pressure measurements when the instrument is operated in the static gas geometry. The ultimate pressure in the chamber is about 5×10^{-7} Torr. However, in the crossed beam geometry mode of operation the background pressure rises to about 2×10^{-5} Torr.

2. *UV/visible spectrometer and photon counting system*

This is an automatic scanning spectrometer made by McPherson Instruments. It has a $f/4.5$ optical system which operates at near normal incidence and spans a spectral region from 50 to 550 nm. This spectral range is covered by two concave 20 cm focal length holographic gratings which have 1200 lines/mm. For the region between 115 to 550 nm a MgF_2 coated grating is used; and for the region between 50 to 550 nm, when extreme UV measurements are made, an osmium coated grating is employed. The typical dispersion of this equipment is about 3.4 nm/mm at 100 nm. The grating is rotated on its axis by a stepping motor which can be controlled by external electrical pulses. Thus, the spectrum can be scanned at a desired speed repeatedly. An electronic

interface between the spectrometer and a multichannel analyzer has been built by our laboratory to store the data at a desired speed. The entrance and exit slit widths and slit heights of this spectrometer can be precisely varied. The change of the slit widths varies the overall wavelength resolution of the spectrometer. The spectrometer is capable of 0.1 nm resolution. However, normally, for the sake of good signal to noise ratio, it is operated at 0.4 nm resolution.

At the exit slit of the spectrometer various photon detectors are placed. At the present time, the entire wavelength region (50 to 550 nm) is covered by two photomultipliers and a spiraltron. The spiraltron covers the spectral range from 50 to 120 nm. One of the photomultipliers has a CsI cathode with a MgF_2 window and is used for the spectral range from 115 to 220 nm. The second photomultiplier has a trialkali cathode and covers a range from 200 to 550 nm. A high sensitivity and very quiet amplifier is used to amplify the output photon pulses for counting purposes. These pulses are stored in a 1024 channel multichannel analyzer. The output of this analyzer is coupled to a computer for data reduction and graphics display.

3. Electronic interface between the collision chamber and the spectrometer

This interface has been built in our laboratory. It synchronizes the channel address in the multichannel analyzer with either the energy of the incident electron beam for the excitation function measurements or the wavelength for spectral scans. Thus, the apparatus can be operated either in the "energy scan" mode or in the "wavelength scan" mode. The synchronization is such that the data can be acquired repeatedly over a fixed interval of energy or wavelength for a long period of time. The whole system is quite reliable and measurements have been made over a period of five days at a time without any measurable distortion in the data.

B. Calibration of the instrument

Two types of standard sources have been used for determining the relative spectral response of the optical system. They are (1) black body standards, and (2) well documented studies of electron impact emissions of N_2 and H_2.

The relative calibration for the long wavelength region from 200 to 550 nm was accomplished by using two standard sources of irradiances. The first source was a deuterium arc lamp with a useful spectral range from 180 to 400 nm. The second source was a quartz–halogen lamp for the spectral range from 300 to 550 nm. The point to point accuracy of relative calibration in this range is better than 10%. The maximum sensitivity of the optical system in the 200 to 550 nm region occured at 280 nm, which was consistent with the quantum efficiency of the photomultiplier tube as the determining sensitivity factor in this wavelength region.

For the short wavelength region from 110 to 210 nm, the relative optical calibration was determined from the molecular branching ratio technique as described by Mumma.[15] This method uses the electron collision chamber with a standard gas, in this case N_2 or H_2, as a target source. For example, the Lyman-Birge-Hopfield system of N_2 together with certain NI multiplets allowed us a calibration from 115 to 190 nm. The relative calibration of the optical system is accurate to 20% in the short wavelength region. In this manner the maximum sensitivity of the short wavelength region was found to occur at 140 nm, which was consistent with the manufacturer's combined characteristics of grating efficiency and photomultiplier quantum efficiency. As a result of this calibration, the absolute response of the optical system from 115 to 550 nm is known to 25% accuracy.

The absolute cross sections for CS_2 were obtained by normalizing to the known cross sections of the $N_2^+(B-X)$, (0, 0) band at 391.4 nm, and Ly-α at 121.57 nm generated by 100 eV electron impact on N_2 and H_2, respectively. The cross section for the 391.4 nm band of N_2^+ was taken to be 1.74×10^{-17} cm^2 measured by Borst and Zipf and agrees with four other independent measurements.[16] For Ly-α the cross section was 1.2×10^{-17} cm^2 measured by several authors with 10% agreement with each other.[17] In order to obtain the absolute value of the cross section for a spectral band of CS_2, the area under the band was measured. Similarly, the area under the 391.4 nm band of N_2^+ or the 121.57 nm line of H was measured. These spectral features were generated under the static gas mode, where the whole chamber was filled, alternately, with CS_2 and N_2 or H_2. The ratio of the two measured areas is given by the following relation:

$$\frac{F_{\lambda1}(CS_2)}{F_{\lambda2}(CAL)}=\frac{G_{\lambda1}}{G_{\lambda2}}\cdot\frac{Q_{\lambda1}(CS_2)}{Q_{\lambda2}(CAL)}\cdot\frac{P_{\lambda1}}{P_{\lambda2}}\cdot\frac{I_{\lambda1}}{I_{\lambda2}}, \tag{1}$$

where $F_{\lambda1}(CS_2)$ and $F_{\lambda2}(CAL)$ are the measured intensities of the CS_2 spectral band and of the $N_2^+(391.4$ nm) band or H(121.57 nm) line, respectively, $G_{\lambda1}$ and $G_{\lambda2}$ are the spectral sensitivities of the optical system at the two wavelengths, $Q_{\lambda1}(CS_2)$ and $Q_{\lambda2}(CAL)$ are the respective excitation cross sections, $P_{\lambda1}$ and $P_{\lambda2}$ are the static gas pressures of CS_2 and N_2 or H_2, respectively, and $I_{\lambda1}$ and $I_{\lambda2}$ are the Faraday cup currents associated with CS_2 and H_2 or N_2, respectively. The ratio $G_{\lambda1}/G_{\lambda2}$ is determined by the method described in the previous paragraphs. The ratio $P_{\lambda1}/P_{\lambda2}$ for the pressures of two gases is obtained by an MKS baratron. This ratio is also checked by the ion guage for consistency. The ratio $I_{\lambda1}/I_{\lambda2}$ was determined by measuring the electron beam currents with a deep Faraday cup held at 40 V potential shown in Fig. 1. Thus, the ratio $Q_{\lambda1}(CS_2)/Q_{\lambda2}(CAL)$ was obtained. The absolute value of $Q_{\lambda1}(CS_2)$ was obtained by multiplying this ratio by the known value of $Q_{\lambda2}(CAL)$.

III. RESULTS

An overall perspective of emissions resulting from CS_2 excitation can be surmized from Figs. 2, 3, and 4, which illustrate, respectively, emissions at 100 eV in the following spectral ranges: (1) VUV, 110–210 nm, (2) middle UV, 240–291 nm, and (3) visible, 430–520

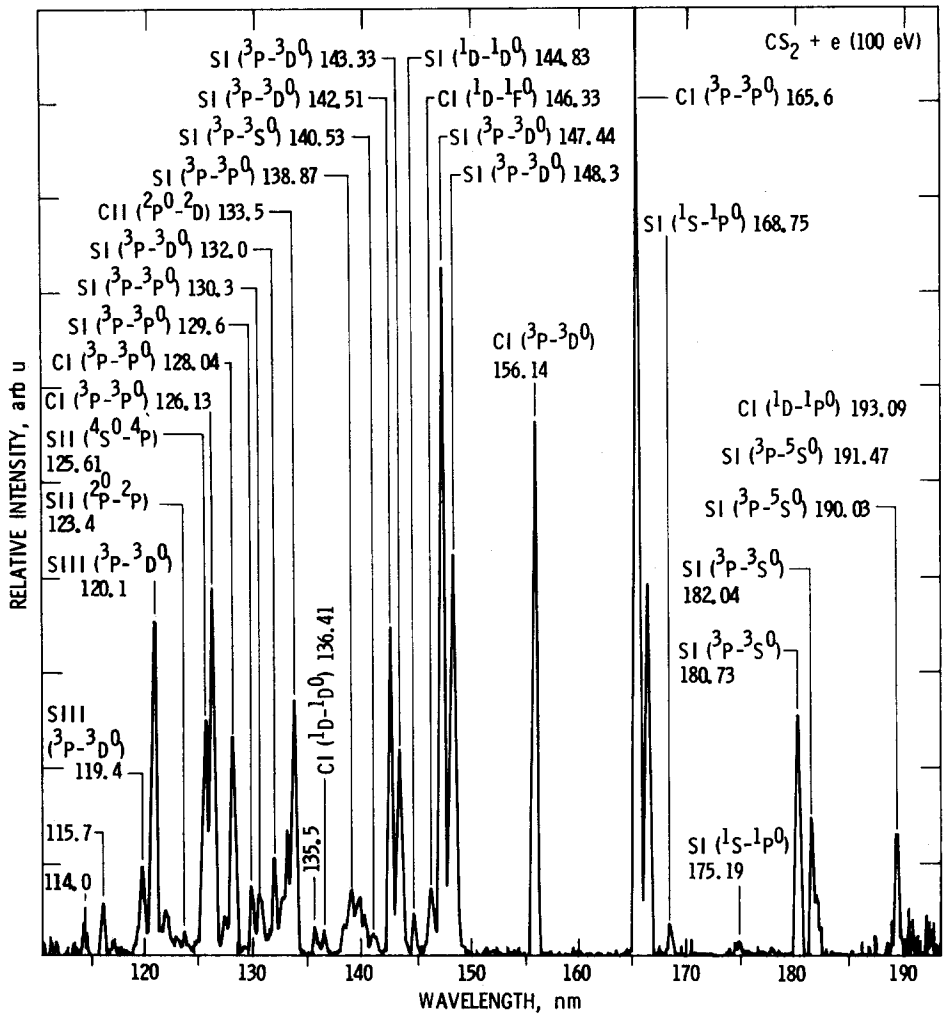

FIG. 2. Calibrated VUV Spectrum of CS_2+e (100 eV). The atomic multiplets are identified from Wiese, Smith, and Glennon.[20] The estimated uncertainty of the relative calibration is 20%. The bandpass of the spectrometer was 0.5 nm.

nm. Between 210 and 240 and between 291 and 430 nm no spectral features were found. This indicates that any emission feature in these two ranges would have a cross section of less than 10^{-19} cm^2. It is clear from a consideration of Figs. 2–4 that the VUV region (110–210 nm) is completely dominated by atomic multiplets. At the same time the middle UV reveals the strong bands at 282.0 and 285.5 nm, which are the strongest transitions from the B state of CS_2^+. Finally, the visible region shows the band system from the A state of CS_2^+. This series of spectra is very analogous in appearance to the spectrum of the isoelectronic linear molecule CO_2, which is also dominated by emissions from its ions in the middle UV and visible and by emissions from atomic species in the VUV.[18]

We show in Fig. 5 a partial energy level diagram of CS_2. This diagram indicates important ionization and dissociation limits for production of ground and excited state products.

In the following we will discuss the three spectral regions in detail.

A. 110 to 210 nm

From the VUV region we list in Table I the observed atomic multiplets[20] and the corresponding cross sections at 100 eV. The strongest emission features are resonance multiplets of CI(^3P–$^3P^0$) at 165.60 nm, SI(^3P–$^3D^0$) at 147.85 nm, and SI(^3P–$^3D^0$) at 142.91 nm with cross sections of 5.1×10^{-18}, 6.4×10^{-18}, and 2.9×10^{-18} cm^2, respectively, at 100 eV electron impact, summed over the multiplet components. Additionally, the resonance lines of singly and doubly ionized sulfur and of singly ionized carbon are observed. In total, a host of carbon and sulfur atomic multiplets are found. These emissions have predicted energy thresholds $T_{\min}$ (dissociation limits given in Fig. 5) of 20±1 eV for a total fragmentation of a molecule into two neutral atoms and one excited atom, either C or S, e.g.,[19,20]

$$CS_2(\tilde{X}\,^1\Sigma_g^+) + e \rightarrow C(^3P) + S(^3P) + S(^3D^0) + e\,, \tag{2}$$

$$S(^3D^0) \rightarrow S(^3P) + h\nu_{142.9\,\mathrm{nm}}\,, \tag{3}$$

$$T_{\min} = \Delta Hf_0^\circ(C) + 2\Delta Hf_0^\circ(S) - \Delta Hf_0^\circ(CS_2) + h\nu_{142.9\,\mathrm{nm}} = 20.60\ \mathrm{eV}\,. \tag{4}$$

Similarly, for fragmentation onto a ground state CS molecule and an excited sulfur atom, we have predicted thresholds (Fig. 5) of 13±1 eV, e.g.,

$$CS_2(\tilde{X}\,^1\Sigma_g^+) + e\, CS(X\,^1\Sigma^+) + S(^3D^0) + e\,, \tag{5}$$

$$S(^3D^0) \rightarrow S(^3P) + h\nu_{147.85\,\mathrm{nm}}\,, \tag{6}$$

$$T_{\min} = \Delta Hf_0^\circ(CS) + \Delta Hf(S) - \Delta Hf_0^\circ(CS_2) + h\nu_{147.85\,\mathrm{nm}}\,, \tag{7}$$

$$T_{\min} = 12.86\ \mathrm{eV}. \tag{8}$$

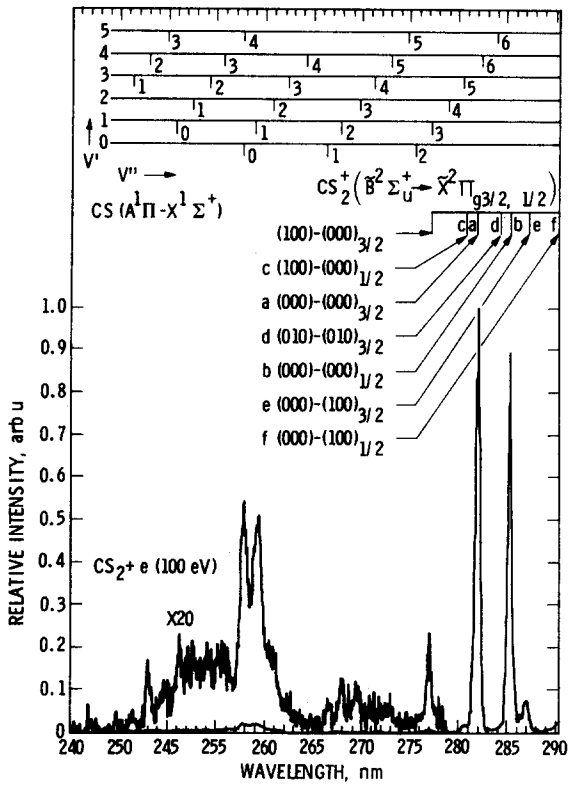

FIG. 3. Calibrated middle UV spectrum of $CS_2 + e$ (100 eV). The CS ($A\,^1\Pi \rightarrow X\,^1\Sigma^+$) band system is identified from Pearse and Gaydon.[22] The CS_2^+ ($B\,^2\Sigma_u^+ \rightarrow X\,^2\Pi_g$) band system is identified from Balfour[4] and the features include the original identification letters designated by Callomon.[21] The bandpass of the instrument is 0.5 nm and the estimated uncertainty of the relative calibration is 10%.

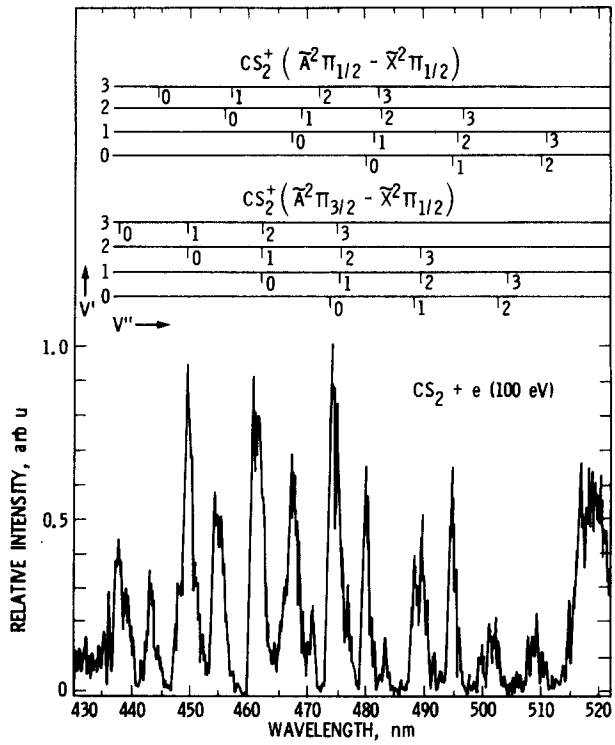

FIG. 4. Calibrated visible spectrum of $CS_2 + e$ (100 eV). The CS_2^+ ($\tilde{A}\,^2\Pi_u \rightarrow {}^2\Pi_g$) band system is identified from Balfour.[4] The estimated uncertainty of the relative calibration is 10%. The bandpass was 1.0 nm.

Additionally, the total cross section at 100 eV summed over all spectral lines in the VUV is 3.6×10^{-17} cm^2.

B. 240 to 291 nm

Perhaps the most important region from the standpoint of large cross sections is the middle UV (240–291 nm). For example, either of the emission bands at 282.0 or 285.5 nm has as large an emission cross section at 100 eV as the entire VUV region. We summarize in Table II the relative strengths of each of the bands of the B state.[4,21] Other bands of the B state found in Refs. 4 and 21 contribute a total of less than 1% to the cross section. The $(000)-(000)_{1/2,3/2}$ transitions represent 90% of the observed intensity. The total cross section of the B state at 100 eV electron impact is found to be 9.0×10^{-17} cm^2. We show in Fig. 6 the

TABLE I. Observed VUV atomic multiplets and cross sections at 100 eV from CS_2.

λ (nm)	Transition[a]	σ (10^{-18} cm^{-2})	λ (nm)	Transition[a]	σ (10^{-18} cm^{-2})[b]
114.0		0.16	142.51	SI($^3P-{}^3D^0$)	1.62
115.7		0.28	143.33	SI($^3P-{}^3D^0$)	1.26
119.4	SIII($^3P-{}^3D^0$)	0.56	144.83	SI($^1D-{}^1D^0$)	0.19
120.1	SIII($^3P-{}^3D^0$)	1.95	146.33	CI($^1D-{}^1D^0$)	0.44
123.4	SII($^2P^0-{}^2P$)	0.14	147.44	SI($^3P-{}^3D^0$)	3.72
125.61	SII($^4S^0-{}^4P$)	3.56	148.3	SI($^3P-{}^3D^0$)	2.64
126.13	CI($^3P-{}^3P^0$)		156.14	CI($^3P-{}^3D^0$)	2.74
128.04	CI($^3P-{}^3P^0$)	1.69	165.6	CI($^3P-{}^3P^0$)	5.09
129.6	SI($^3P-{}^3P^0$)	0.32	166.67	SI($^1D-{}^1D^0$)	1.92
130.3	SI($^3P-{}^3P^0$)	0.39	168.75	SI($^1S-{}^1P^0$)	0.15
132.0	SI($^3P-{}^3D^0$)	1.47	175.19	CI($^1S-{}^1P^0$)	0.08
133.5	CII($^2P^0-{}^2D$)	1.36	180.73	SI($^3P-{}^3S^0$)	1.15
135.6		0.15	182.04	SI($^3P-{}^3S^0$)	0.84
136.41	CI($^1D-{}^1D^0$)	0.14	190.03	SI($^3P-{}^5S^0$)	0.65
138.87	SI($^3P-{}^3P^0$)	1.15	191.47	SI($^3P-{}^5S^0$)	0.13
140.53	SI($^3P-{}^3S^0$)	0.16	Total all atomic 114.0–192.0 nm multiplets		36.10

[a]Identifications from Ref. 20.

[b]The cross section values are estimated to have an experimental uncertainty of 25%.

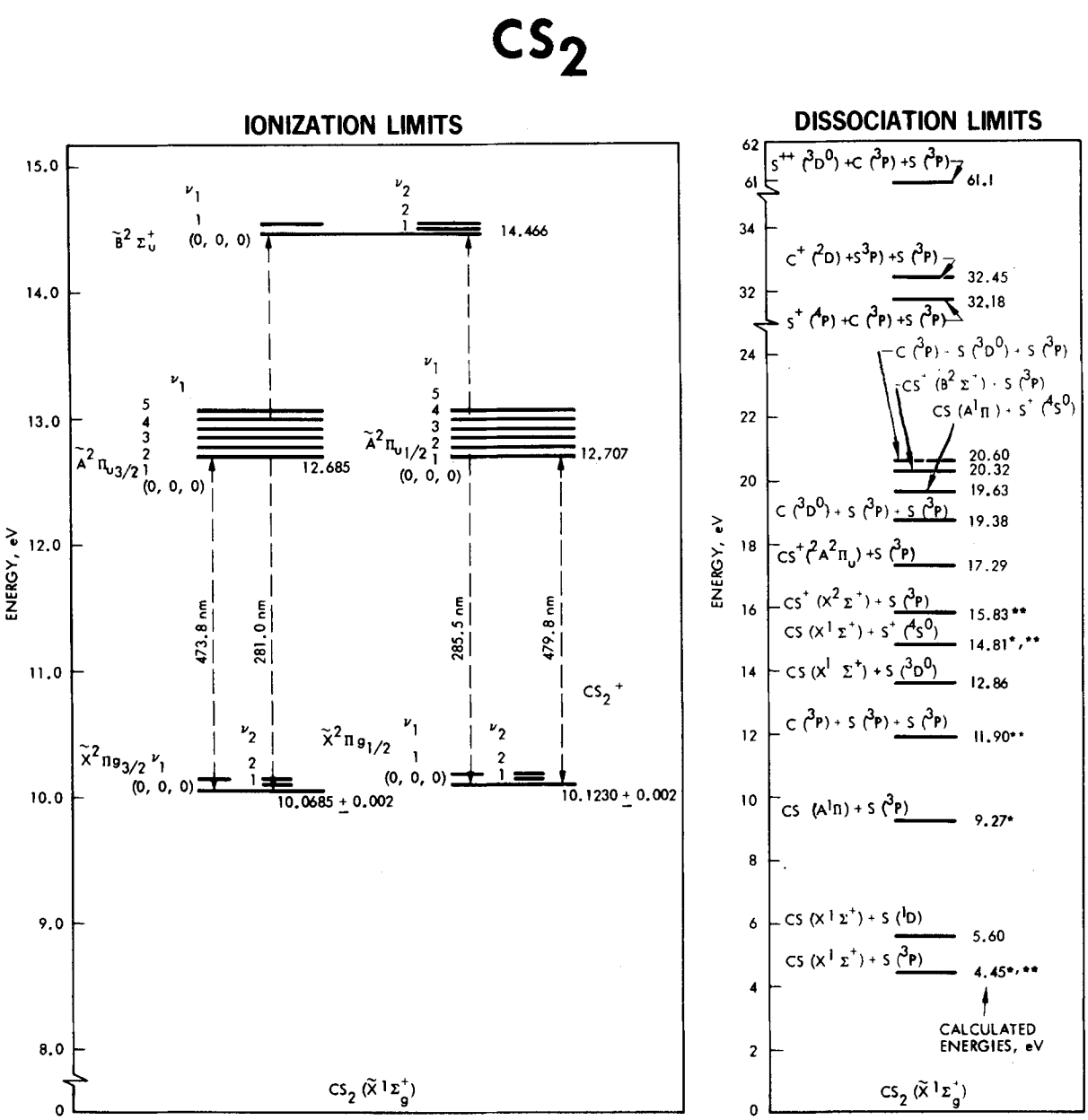

FIG. 5. A plot of important dissociation limits and ionization potentials of CS_2. The heats of formation of ground state products are taken from Rosenstock *et al.*[19]; the states of excited C, S, C^+, S^+, and S^{++} atoms (ions) are taken from Wiese *et al.*[20] and the ionization potential of CS_2 is from Ono *et al.*[8] Thresholds which have been experimentally measured are indicated by a *.[8,24] Threshold energies marked with ** represent products in ground states. The threshold values for the CS^+ ions are taken from Ref. 23.

emission cross section of the B state as a function of incident electron energy between 0 and 125 eV. Note the rapid rise in cross section with energy and the broad maximum from 40–100 eV. We measured both the 282.0 and 285.5 nm emission cross sections and found them to have the same energy dependence.

In this spectral region, the band system of $CS(A\,^1\Pi - X\,^1\Sigma^+)$ was also found. This system is seen more clearly in Fig. 7 at 20 eV than in Fig. 2 at 100 eV. It results from the dissociative excitation and has been previously studied by Lee and Judge.[12] The band heads were found in Pearse and Gaydon.[22] Although there are some differences in detail, the observed spectra at either 20 or 100 eV agree in relative intensities for the

TABLE II. B state vibrational cross sections.

λ (nm)	Transition ($\tilde{B}\,^2\Sigma_u^+ \rightarrow \tilde{X}\,^2\Pi_g$)	% of cross section of B state
277.3	$(100)-(000)_{3/2}$	0.51
280.7	$(100)-(000)_{1/2}$	1.4
280.9	$(010)-(010)_{1/2}$	
282.0	$(000)-(000)_{3/2}$	46.7
284.4	$(010)-(010)_{3/2}$	0.74
285.5	$(000)-(000)_{1/2}$	42.9
287.0	$(000)-(100)_{3/2}$	5.4
290.7	$(000)-(100)_{1/2}$	1.4

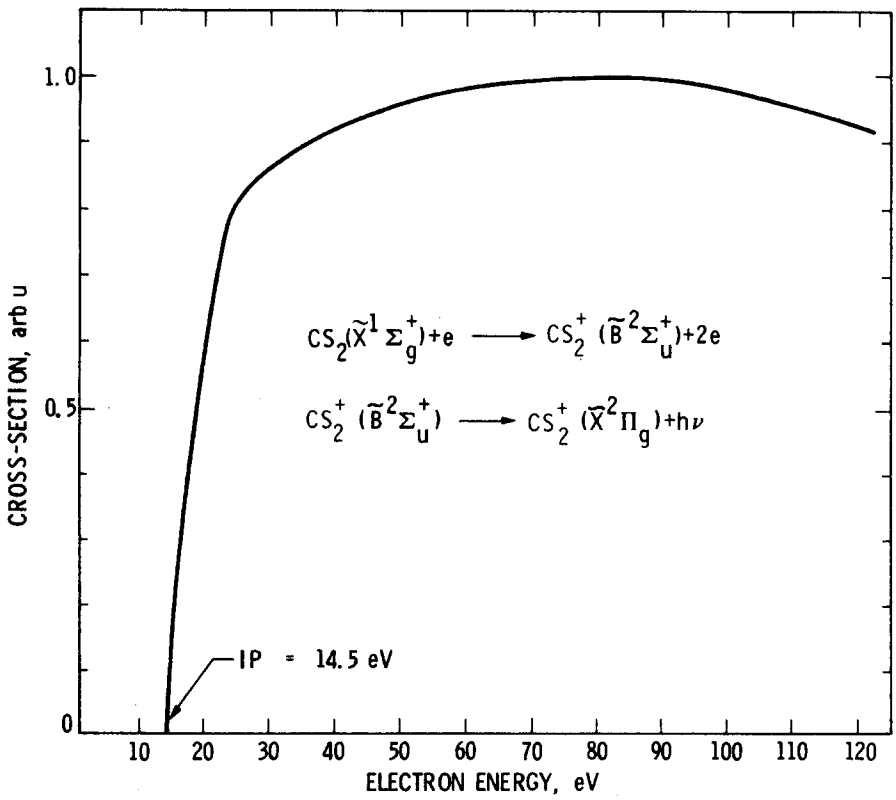

FIG. 6. Emission cross section of the $\tilde{B}^2\Sigma_u^+ \rightarrow \tilde{X}\Pi_g$ transition of CS_2^+ by electron impact.

various bands with the spectrum of Lee and Judge. Additionally, there is no evidence in this spectral region of the recently discovered weak band system $CS^+(B^2\Sigma^+ \rightarrow X^2\Sigma^+)$.[23]

We show in Fig. 8 the emission cross section of the $CS(A^1\Pi)$ state which is found to have a cross section, at 100 eV, of 1.2×10^{-17} cm^2. It has the unusual characteristic of having double maxima at 12 ± 2 and 25 ± 3 eV. The first peak is characteristic of a spin-forbidden process produced in photodissociative excitation of CS_2[24]:

$$CS_2(\tilde{X}^1\Sigma_g^+) + e \rightarrow CS(A^1\Pi) + S(^3P) + e\,. \quad (9)$$

Thus, the repulsive intermediate state of CS_2^* is probably a triplet level. The other broad peak is due either to an additional dissociative process, probably allowed, or to a dissociative ionization process, e.g.,

$$CS_2(\tilde{X}^1\Sigma_g^+) + e \rightarrow CS(A^1\Pi) + S(^1D) + e\,, \quad (10)$$

or

$$CS_2(\tilde{X}^1\Sigma_g^+) + e \rightarrow CS(A^1\Pi) + S^+(^4S^0) + 2e\,. \quad (11)$$

There are several observed Rydberg series at 10 to 11 eV.[25] Perhaps these states predissociate as indicated by

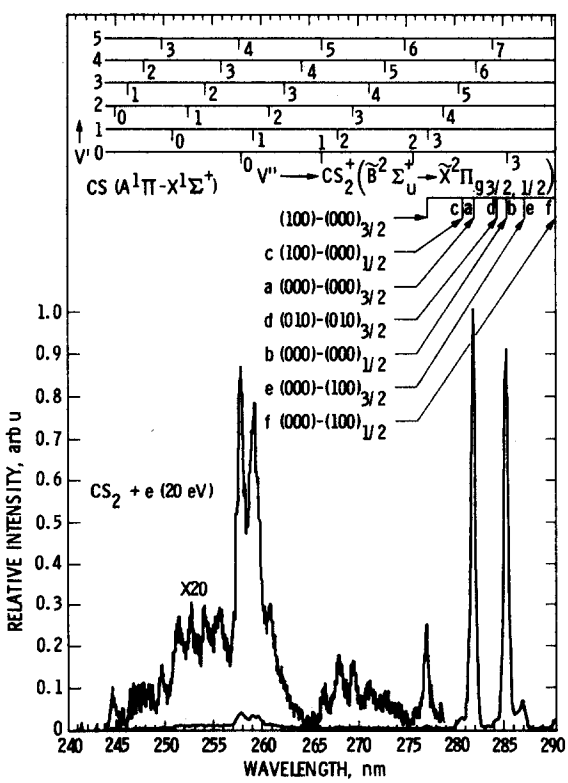

FIG. 7. Calibrated middle UV spectrum of CS_2+e (20 eV).

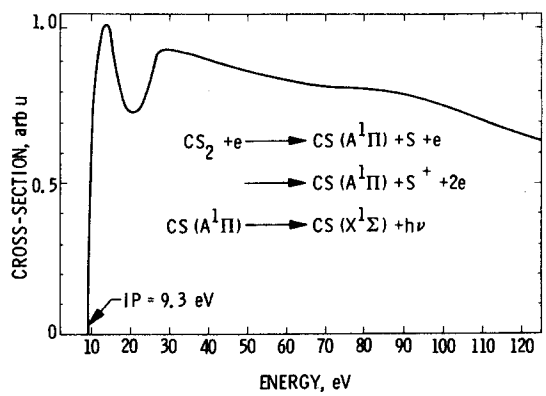

FIG. 8. Emission cross section of the $A^1\Pi \rightarrow X^1\Sigma^+$ transition of CS_2^* by electron impact.

TABLE III. Comparison of CS_2 emission cross sections at 100 eV.

Transition	Absolute cross section at 100 eV (cm^2)[a]
$CS_2^+(\tilde{B}\,^2\Sigma_u^+ \rightarrow \tilde{X}\,^2\Pi_g)$	9.0×10^{-17}
$CS_2^+(\tilde{A}\,^2\Pi_u \rightarrow \tilde{X}\,^2\Pi_g)$	3.1×10^{-17}
$CS(A\,^1\Pi \rightarrow X\,^1\Sigma^+)$	1.2×10^{-17}
VUV atomic multiplets (110–200 nm)	3.6×10^{-17}

[a]The cross section values are estimated to have an experimental uncertainty of 25%.

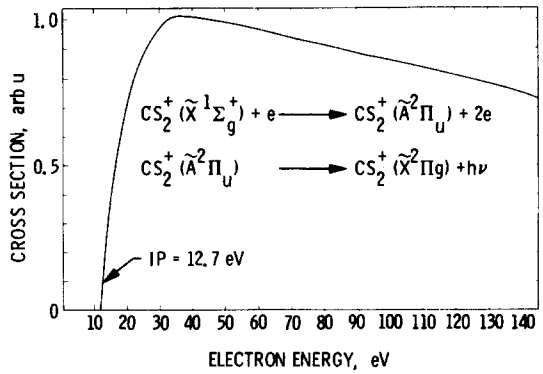

FIG. 9. Emission cross section of the $\tilde{A}\,^2\Pi_g \rightarrow \tilde{X}\,^2\Pi_g$ transition of CS_2^+ by electron impact.

the first process. As an example of the latter process, Dibeler and Walker[8] have observed dissociative photoionization (see Fig. 5) with a threshold of 14.81 eV for ground state products. We have indicated a calculated threshold for a $CS(A\,^1\Pi)$ excited state product of 19.63 eV in Fig. 5.

C. 430 to 510 nm

The final spectral region consists of the bands from the $CS_2^+(A\,^2\Pi_u \rightarrow X\,^2\Pi_g)$ transition. The band heads have been identified by Balfour.[4] The cross section for the transition is indicated in Fig. 9. The normalizing value to this curve occurs at 100 eV, where we have measured a value of 3.1×10^{-17} cm^2. The spectrum shown in Fig. 3 is similar to that observed from photon impact fluorescence studies.[13] In the fluorescence study the complete band system was observed which extends to 560 nm. The published photon impact fluorescence spectrum was used in the range 520 to 560 nm to provide the fractional contribution to the total electronic cross section in the wavelength range not measured in this experiment.

IV. DISCUSSION

We summarize in Table III the important emission cross sections over the wavelength range 110 to 510 nm. From this table it is interesting to note that the combined cross section of the 282.0 and 285.5 nm doublet

TABLE IV. Franck–Condon factors and relative intensities for the $CS(A\,^1\Pi \rightarrow X\,^1\Sigma^+)$ band system.

Bands (v', v'')	λ (nm)	$F_{v'v''}$[a]	$q_{v'v''}$[b] e impact	Photon impact[d]	Calc.[e]
(0,0)	257.56	1.12	0.85	0.78	0.77
(0,1)	266.26	0.12	0.10	0.15	0.19
(0,2)	275.47	0.05	0.05	0.06	0.03
(1,0)	250.73	0.33	0.19	0.13	0.20
(1,1)	258.96	1.0	0.62	0.61	0.40
(1,2)	267.70	0.21	0.14	0.20	0.30
(1,3)[c]	276.92	0.07	0.04	0.05	0.08
(2,0)	244.48	0.08	0.06	0.03	0.03
(2,1)	252.32	0.37	0.32	0.25	0.31
(2,2)	260.59	0.36	0.34	0.37	0.15
(2,3)	269.32	0.19	0.20	0.29	0.33
(2,4)[c]	278.57	0.06	0.07	0.06	0.14
(3,1)	246.02	0.08	0.08	0.08	0.08
(3,2)	253.87	0.38	0.41	0.33	0.34
(3,3)	262.16	0.18	0.22	0.16	0.02
(3,4)	270.89	0.12	0.16	0.31	0.28
(3,5)	280.15	0.09	0.13	0.14	0.20
(4,2)	247.70	0.09	0.14	0.12	0.14
(4,3)	255.58	0.34	0.59	0.52	0.29
(4,4)	263.89	0.05	0.09	0.06	0.003
(4,5)	272.67	0.08	0.17	0.29	0.18

[a]Intensities normalized to the (1,1) band.
[b]The sum of Franck–Condon factors over v'' is set equal to 1 for each v'.
[c]Relative intensities taken from Ref. 12.
[d]Reference 12.
[e]Reference 28.

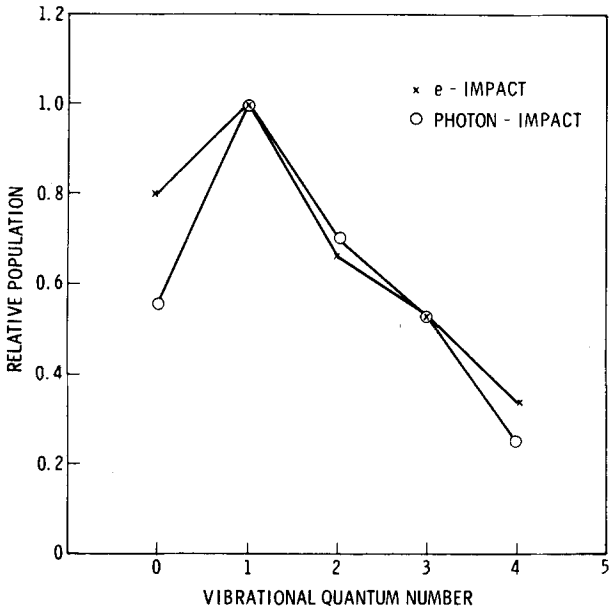

FIG. 10. The measured variation in population of the vibrational levels of $A\,^1\Pi$ state of electron impact excitation of CS_2.

(90% of the B state cross section) is larger than all other emission cross sections combined. As we have mentioned earlier, this situation is similar to the electron emission cross section results obtained for CO_2. For example, Ajello[18] found the spectrum in the UV also to be dominated by electronic transitions of the CO_2^+ ion with no observed transitions from the neutral molecule. By way of comparison, the total emission cross section of the A and B states of CO_2^+ is 1.3×10^{-16} cm^2, which compares favorably to the total emission cross section of about 1.2×10^{-16} cm^2 for the A and B states of CS_2^+ found in this work. For CO_2, the total ionization cross section[26] at 100 eV is 3.5×10^{-16} cm^2, which implies that 1/3 of the CO_2^+ ions produced at 100 eV are in excited states. However, in the case of CS_2 an important difference arises since the ionization excitation cross section of the B state is much larger than the ionization excitation cross section of the lower lying A state. A final point of comparison at this stage would be to compare the cross section for the excited ionization states of CS_2^+ to the total ionization cross section. However, the total ionization cross section for CS_2 has not been experimentally determined. The only ionization study which includes the ground state of CS_2^+ are the He (58.4 nm) photoelectron spectroscopy studies of CS_2.[27] In the photoelectron measurements at 21.2 eV the relative ratio of $X:A:B\cong2:1:1$ compared to our 100 eV ratio for electron impact of $A:B\cong1:3$. However, we do not expect correlation between these two ionization experiments.

Another important comparison is to study the relative intensity differences of the $CS(A\,^1\Pi\rightarrow X\,^1\Sigma^+)$ transition produced by electron impact and photon impact. For this purpose we have assembled Table IV, which shows the relative intensities $F_{v'v''}$ produced by 20 eV electrons and the experimentally derived Franck–Condon factors. The relationship between $F_{v'v''}$ and $q_{v'v''}$ makes use of the equation

$$F_{v'v''}=\frac{CN_{v'}R^2_{ev'v''}q_{v'v''}}{\lambda^3_{v'v''}}\ , \tag{12}$$

where C is a constant, $N_{v'}$ is the population density in level v', $R^2_{ev'v''}$ is the electronic transition moment (assumed to be a constant), $q_{v'v''}$ is the Franck–Condon factor, and $\lambda_{v'v''}$ is the band head wavelength. For comparison we also list the Franck–Condon factors from 10 eV photon impact[12] and the Franck–Condon factors for direct excitation of CS based on theoretical considerations.[28] In general, the photon and electron impact values agree but are substantially different than the theoretical values.

From the measured intensities the relative vibrational populations are determined and are shown in Fig. 10. It is found that a populated inversion exists between $v'=1$ and $v'=0$, although not as large as produced by 10 eV photon impact. The population distribution in the vibrational levels of a dissociation fragment is of theoretical importance for developing dissociation models.[10,11]

There have been no previous VUV emission spectra of CS_2 from either electron or photon impact. However, several cometary spectra[1–3] have been published which include weak features, some of which have been identified as CI and SI features. We suggest that several unidentified features and several features previously identified solely as the CO fourth positive system may include additional contributions from the CI and SI multiplets at the wavelengths observed in this experiment.

Furthermore, the IUE satellite has observed cometary emission[2] from the $CS(A\,^1\Pi\rightarrow X\,^1\Sigma^+)$ band system including several of the features from this band system identified in our study. The absence of the strong 282.0 and 285.5 nm CS_2^+ emissions in the cometary spectra suggests that the CS emissions come directly from fluorescence excitation of CS.

ACKNOWLEDGMENTS

We thank Dr. Jacques Blamont for suggesting this project and for stimulating disucssions regarding cometary spectra. We also thank Mr. William Simms for designing and building the electronic interface.

[1] M. W. Jackson, J. Rahe, B. Donn, A. M. Smith, H. U. Keller, P. Benevenuti, A. H. Delsemme, and T. Owen, Astron. Astrophys. 73, L7 (1979); A. M. Smith, T. P. Stecker, and L. Casswell, Astrophys. J. 242, 402 (1980).
[2] W. M. Jackson, J. Halpern, P. D. Feldman, and J. Rahe, in *Proceedings of the Universe at Ultraviolet Wavelengths: The First Two years of* IUE, (Goddard Space Flight Center, Greenbelt, 1979).
[3] P. Feldman, Am. Sci. 65, 298 (1977); P. Feldman and W. H. Brune, Astrophys. J. 209, 45 (1976).
[4] W. J. Balfour, Can. J. Phys. 54, 1969 (1976).
[5] W. H. Smith, J. Quant. Spectrosc. Radiat. Transfer 9, 1191 (1969).
[6] M. Larzilliere and H. Damony, Can. J. Phys. 56, 1150 (1978).
[7] Y. Ono, S. H. Linn, H. F. Prest, M. E. Gress, and C. Y. Ng, J. Chem. Phys. 73, 2523 (1980).
[8] V. H. Dibeler and J. A. Walker, J. Opt. Soc. Am. 57, 1007

(1967).
[9]V. E. Bondybey and J. H. English, J. Chem. Phys. **73**, 3098 (1980).
[10]J. E. Butler, W. Drozdoski, and J. R. McDonald, Chem. Phys. **50**, 413 (1980).
[11]S. C. Yang, A. Freedman, M. Kawasaki, and B. Bersohn, J. Chem. Phys. **72**, 4058 (1980).
[12]L. E. Lee and D. L. Judge, J. Chem. Phys. **63**, 2782 (1975).
[13]L. C. Lee, D. L. Judge, and M. Ogawa, Can. J. Phys. **53**, 1861 (1975).
[14]S. K. Srivastava, J. Ajello, and J. Watkins (to be published).
[15]M. J. Mumma, J. Opt. Soc. Am. **62**, 1459 (1972).
[16]W. L. Borst and E. C. Zipf, Phys. Rev. A **1**, 183 (1970).
[17]M. J. Mumma and E. C. Zipf, J. Chem. Phys. **55**, 1661 (1971).
[18]J. M. Ajello, J. Chem. Phys. **55**, 1369 (1971).
[19]H. M. Rosenstock, K. Draxl, B. W. Sterne, and J. T. Herron, J. Phys. Chem. Ref. Data **6**, Suppl. 1 (1977).
[20]W. L. Wiese, M. W. Smith, and B. M. Glennon, "Atomic transition probabilities—Hydrogen through neon," Natl. Stand. Ref. Data Ser. Natl. Bur. Stand. **4**, 30 (1966).
[21]J. H. Callomon, Proc. R. Soc. London Ser. A **244**, 220 (1958).
[22]R. W. B. Pearse and A. G. Gaydon, *The Identification of Molecular Spectra* (Wiley, New York, 1976), p. 120.
[23]M. Tsuji, H. Obase, and Y. Nishimura, J. Chem. Phys. **73**, 2575 (1980); K. T. Wu and A. J. Yencha, Chem. Phys. Lett. **67**, 134 (1979).
[24]H. Okabe, J. Chem. Phys. **56**, 4381 (1972); S. V. Filseth, *Advances in Photochemistry* (Wiley, New York, 1977), Vol. 10, pp. 42–47.
[25]J. W. Rabalais, J. M. McDonald, V. Scherr, and S. P. McGlynn, Chem. Rev. **71**, 73 (1971).
[26]D. Rapp and P. Englander-Golden, J. Chem. Phys. **43**, 1464 (1965).
[27]D. W. Turner, C. Baker, A. D. Baker, and G. R. Brundle, *Molecular Photoelectron Spectroscopy* (Wiley-Interscience, London, 1967), p. 98.
[28]P. Felenbok, Proc. Phys. Soc. London **86**, 676 (1965).